JfM PAPERS

Coupled continuous time random walks for dispersion in spatio-temporal random flows

Marco Dentz[1] and **Daniel Robert Lester**[2]

[1]Spanish National Research Council (IDAEA-CSIC), Barcelona, Spain
[2]School of Engineering, RMIT University, 3000 Melbourne, Australia
Corresponding author: Marco Dentz, marco.dentz@csic.es

Dispersion in spatio-temporal random flows is dominated by the competition between spatial and temporal velocity resets along particle paths. This competition admits a range of normal and anomalous dispersion behaviours characterised by the Kubo number, which compares the relative strength of spatial and temporal velocity resets. To shed light on these behaviours, we develop a Lagrangian stochastic approach for particle motion in spatio-temporally fluctuating flow fields. For space–time separable flows, particle motion is mapped onto a continuous time random walk (CTRW) for steady flow in warped time, which enables the upscaling and prediction of the large-scale dispersion behaviour. For non-separable flows, we measure Lagrangian velocities in terms of a new sampling variable, the average number of velocity transitions (both temporal and spatial) along pathlines, which renders the velocity series Markovian. Based on this, we derive a Lagrangian stochastic model that represents particle motion as a coupled space–time random walk, that is, a CTRW for which the space and time increments are intrinsically coupled. This approach sheds light on the fundamental mechanisms of particle motion in space–time variable flows, and allows for its systematic quantification. Furthermore, these results indicate that alternative strategies for the analysis of Lagrangian velocity data using new sampling variables may facilitate the identification of (hidden) Markov models, and enable the development of reduced-order models for otherwise complex particle dynamics.

Key words: porous media, dispersion, intermittency

1. Introduction

The understanding of particle motion in fluctuating flow fields plays a central role for the qualitative and quantitative assessment of tracer migration and hydrodynamic dispersion

(Saffman 1959; Dagan 1989), anomalous transport patterns (de Anna *et al.* 2013), pair dispersion (Shlesinger *et al.* 1987; Sokolov *et al.* 2000), fluid deformation (Dentz *et al.* 2016b; Lester *et al.* 2018), and the mechanisms of stirring and mixing (Villermaux 2019; Dentz *et al.* 2023), among others. Classical Lagrangian stochastic models for transport in fluctuating flow fields model the impact of velocity fluctuations in terms of Markov models for the time series of Lagrangian velocities (Pope 2000). These approaches assume that Lagrangian velocity series are characterised by a single correlation time scale, or, in other words, that they can be quantified by a temporal Markov process.

For particle motion in steady random flow fields, this is in general no longer true, because the velocity correlation time is set by the local flow velocities, which are characterised by a characteristic correlation length scale ℓ_c of the steady velocity field. That is, broad distributions of flow velocities imply broad distributions of characteristic correlation times, which manifest as strong (power-law) temporal velocity correlation and statistical non-stationarity. In fact, particle dispersion in steady spatial random flows is caused by the motion of particles at spatially correlated velocities and random velocity changes after periods of time that correspond to the advection time over a correlation length by the local flow velocity (Saffman 1959). The evolution of particle velocities can be described by a single correlation length scale, that is, they describe a Markov process when sampled equidistantly along streamlines (Dentz *et al.* 2016a). The corresponding particle motion has been quantified in the continuous time random walk (CTRW) framework (Berkowitz *et al.* 2006; Dentz *et al.* 2016a). These ideas have been used for the modelling and interpretation of solute transport in heterogeneous porous media from the pore to the regional scales (Berkowitz *et al.* 2006; Morales *et al.* 2017; Comolli *et al.* 2019; Hyman *et al.* 2019; Puyguiraud *et al.* 2019b; Sherman *et al.* 2021).

Conversely, particle transport in spatio-temporal random flows evolves due to periods of motion at slowly varying correlated velocities, and random transitions between flow velocities triggered by either spatial or temporal decorrelation. That is, there is a competition between spatial and temporal velocity reset that can be characterised by the Kubo number (Kubo 1962; Krommes & Smith 1987) as the ratio $\kappa = \tau_c/\tau_v$ between the intrinsic fluctuation time scale τ_c of the flow and the advection time scale $\tau_v = \ell_c/\overline{u}$, where $\overline{u}$ denotes a mean flow velocity. Equivalently, $\kappa = \overline{u}\tau_c/\ell_c$ compares the characteristic length ℓ_c with the travel distance $\overline{u}\tau_c$ during a fluctuation period. Thus the Kubo number characterises the relative frequency of velocity reset along a pathline by temporal and spatial flow variability. For $\kappa > 1$, spatial reset is more frequent than temporal, and vice versa for $\kappa < 1$. Sokolov *et al.* (2000) refer to the Kubo number as a flow persistence parameter, which for pair dispersion in the Richardson regime determines whether particle motion is diffusive in character ($\kappa < 1$) or ballistic ($\kappa > 1$). In this context, Levy walks have been used to represent ballistic motion on all scales (Shlesinger *et al.* 1987; Sokolov *et al.* 2000; Thalabard *et al.* 2014). The Levy walk picture emerges from the observation that both velocity correlation time and length evolve as a power law with interparticle distance (Sokolov *et al.* 2000). For particle motion in porous media under temporally variable flow conditions, Nissan *et al.* (2017) and Elhanati *et al.* (2023) use a CTRW approach that accounts for temporal velocity changes along fixed travel distances by adjusting particle travel times. This approach is then used for the interpretation of tracer data from column experiments under temporal flow variability. These authors find that tracer breakthrough curves show a similar tailing behaviour as under steady flow conditions. This observation can be rationalised in the context of the models presented in this paper. Engdahl & Aquino (2022) explore algorithms to accommodate temporal flow fluctuations in spatial Markov models for particle velocities in porous media flows. These authors focus on scenarios of slow temporal flow variation and fast propagation of

velocity changes, and discuss different protocols for the updating of velocity statistics and particle position and time. They emphasise the complexity of upscaling particle motion in situations where spatial and temporal flow decorrelation are competing.

In fact, although these spatial and temporal processes may be Markovian individually, the combined Lagrangian velocity evolution along trajectories in unsteady flow may no longer be so in space or time if the Kubo number κ that characterises the ratio of spatial to temporal decorrelation rates is neither $\kappa \gg 1$ nor $\kappa \ll 1$. This inherent intermittency of Lagrangian velocity fluctuations is characteristic of a wide range of spatio-temporally fluctuating flows. In this paper, we discuss transport in two types of spatio-temporally fluctuating flows. The first type is characterised by intrinsically coupled non-separable space–time fluctuations. For the second type, the space and time fluctuating contributions are separable, i.e. space–time coupling is weak. We show that the latter case can be mapped onto a CTRW for steady flow in warped time, which allows for the upscaling and prediction of the large scale dispersion behaviour. This result provides a theoretical foundation for the observations of Nissan *et al.* (2017) and Elhanati *et al.* (2023) in transient porous media flows. For the non-separable velocity field, we develop a fully coupled CTRW approach, which renders the velocity process Markovian as a function of a new sampling variable that counts the number of velocity transitions (both temporal and spatial) along pathlines.

The paper is organised as follows. Section 2 provides some preliminary remarks on transport in spatio-temporally fluctuating non-separable and separable flow fields, and recalls the CTRW approach for particle motion in steady random flows. Section 3 discusses particle motion in non-separable space–time variable flow. It systematically quantifies the competition between spatial and temporal velocity resetting by introducing a new sampling variable, and analyses the corresponding Lagrangian velocity statistics. Based on this, it derives a novel coupled CTRW approach, which is compared against numerical simulations of particle dispersion in synthetic random flows at different Kubo numbers. Section 4 analyses particle motion in space–time separable random flow fields using a steady CTRW approach in warped time, whose predictions are compared to numerical simulations at different Kubo numbers.

2. Preliminary remarks

We consider particle motion in temporally and spatially variable velocity fields $\mathbf{u}(\mathbf{x}, t)$ as described by the kinematic equation

$$\frac{\mathrm{d}\mathbf{x}(t, \mathbf{a})}{\mathrm{d}t} = \mathbf{u}[\mathbf{x}(t, \mathbf{a}), t], \tag{2.1}$$

where $\mathbf{x}(t = 0, \mathbf{a}) = \mathbf{a}$ is the initial particle position. The velocity field $\mathbf{u}(\mathbf{x}, t)$ is assumed to be divergence-free. It is represented as a realisation of a spatio-temporal random field that decorrelates on the length scale ℓ_c and on the time scale τ_c. The ensemble mean velocity is constant and aligned with the one-direction of the coordinate system, $\langle u_i(\mathbf{x}, t) \rangle = \overline{u} \delta_{i1}$, where the angular brackets denote the ensemble average. The distance $s(t)$ travelled along a pathline is given by

$$\frac{\mathrm{d}s(t, \mathbf{a})}{\mathrm{d}t} = v_t(t, \mathbf{a}), \tag{2.2}$$

where we defined the time-Lagrangian speed $v_t(t, \mathbf{a}) = |\mathbf{u}[\mathbf{x}(t, \mathbf{a}), t]|$. Its distribution is obtained by sampling over fluid particles as

$$p_\ell(v, t) = \lim_{V_0 \to \infty} \frac{1}{V_0} \int_{\Omega_0} \mathrm{d}\mathbf{a} \, \delta[v - v_t(t, \mathbf{a})], \tag{2.3}$$

where Ω_0 denotes the source region. Similarly, the distribution of Eulerian flow speeds is defined by spatial sampling as

$$p_e(v, t) = \lim_{V \to \infty} \frac{1}{V} \int_\Omega \mathrm{d}\mathbf{x}\, \delta[v - |\mathbf{u}(\mathbf{x}, t)|], \tag{2.4}$$

where Ω is the map of Ω_0 through the mapping $\mathbf{a} \to \mathbf{x}(t, \mathbf{a})$. Due to the solenoidal character of the flow field, we have $p_e(v, t) = p_\ell(v, t)$.

We consider two different types of space–time variability. First, we consider the case of an intrinsically coupled space–time velocity field, and second, that of a separable velocity field. We do not consider simple flow reversals and thus exclude memory artefacts along pathlines. In the following, we specify the ergodic properties of the velocity fields under consideration, and briefly recall the stochastic modelling of particle motion in steady random velocity fields, which corresponds to the limit $\kappa \to \infty$.

2.1. *Ergodicity assumptions*

In the following, we discuss the properties that we assume to hold for the space–time random flows underlying the developments in the remainder of the paper.

2.1.1. *Non-separable spatio-temporally fluctuating velocity fields*
For the non-separable velocity fields under consideration here, the space and time fluctuations are intrinsically coupled. We assume that the velocity fields are space–time ergodic; that is, the same statistics are explored by spatial or temporal sampling, which in turn are equal to the ensemble statistics, i.e.

$$p_e(v) = \lim_{V \to \infty} \frac{1}{V} \int_\Omega \mathrm{d}\mathbf{x}\, \delta[v - |\mathbf{u}(\mathbf{x}, t)|] = \lim_{T \to \infty} \frac{1}{T} \int_0^T \mathrm{d}t\, \delta[v - |\mathbf{u}(\mathbf{x}, t)|], \tag{2.5}$$

where $p_e(v)$ denotes the Eulerian speed distribution. Ergodicity is typically assumed for three-dimensional turbulent flows (Frisch 1995), which is supported by direct numerical simulations (Galanti & Tsinober 2004; Djenidi *et al.* 2013). In other words, this property means that temporal sampling at a fixed position gives the same statistics as spatial sampling at a fixed time, which requires that the autocorrelation function of the flow field is short-range correlated in both space and time, and that the spatial and temporal velocity resets are independent. The correlation length and time are denoted by ℓ_c and τ_c. This implies that as a particle moves along a streamline, its velocity may change due to the spatial variability of flow on the scale ℓ_c, or reset due to the temporal variability on the time scale τ_c.

Furthermore, we assume Lagrangian ergodicity, that is, the statistics of the speeds sampled along a single pathline is equal to the ensemble statistics as

$$p_t(v) \equiv \lim_{T \to \infty} \frac{1}{T} \int_0^T \mathrm{d}t\, \delta[v - v_t(t, \mathbf{a})] = p_\ell(v) \equiv \lim_{V_0 \to \infty} \int_{\Omega_0} \mathrm{d}\mathbf{a}\, \delta[v - v_t(t, \mathbf{a})], \tag{2.6}$$

where $p_t(v)$ denotes the distribution of speeds sampled along a trajectory, and $p_\ell(v)$ the distribution of speeds sampled between particles. Each time the velocity is reset along a pathline, by either spatial or temporal fluctuations, the velocity is sampled from the same distribution, which is in general not equal to the Eulerian distribution. We consider volume-conserving flow, that is, $\nabla \cdot \mathbf{u}(\mathbf{x}, t) = 0$ and therefore $p_e(v) = p_\ell(v)$. In §3, we discuss in detail the relation between Eulerian and Lagrangian velocity statistics, and the velocity statistics during resetting along streamlines. In the following, we set $\mathbf{x}(t) = \mathbf{x}(t, \mathbf{a})$ for compactness of notation, and omit the label $\mathbf{a}$ in the Lagrangian quantities.

In general, the ergodicity of Lagrangian velocities may be related to Lagrangian coherent structures (Haller 2015), which can delineate ergodic and non-ergodic flow regions. Temporal variability in the Eulerian velocity field admits a variety of possible Lagrangian dynamics, which govern advective transport and divide the Lagrangian domain into topologically distinct regions with different flow characteristics according to their type (hyperbolic, elliptic or parabolic). As these topological features can be open or closed, and involve different mixing dynamics, they may determine the ergodicity of Lagrangian velocities.

2.1.2. *Separable spatio-temporally fluctuating velocity fields*

We consider now the case that the velocity field $\mathbf{u}(\mathbf{x}, t)$ is space–time separable, with spatially fluctuating velocity $\mathbf{u}(\mathbf{x})$ and temporally fluctuating forcing $\phi(t)$, i.e.

$$\mathbf{u}(\mathbf{x}, t) = \mathbf{u}(\mathbf{x})\,\phi(t). \tag{2.7}$$

This type of velocity field occurs in low Reynolds number flows through non-deformable porous media. Temporal flow fluctuations, either natural or engineered, have been shown to lead to enhanced dispersion and broader residence time distributions than in steady flow (Rehfeldt & Gelhar 1992; Cirpka & Attinger 2003; de Dreuzy *et al.* 2012; Neupauer *et al.* 2014) subject to temporally fluctuating boundary conditions. The specific form (2.7) corresponds to scenarios of temporal flow fluctuations in the streamwise direction as studied in the laboratory experiments by Nissan *et al.* (2017) and Elhanati *et al.* (2023). This type of flow field in general does not display spatio-temporal ergodicity as defined in (2.5), as can be checked easily. Here, we assume that $\mathbf{u}(\mathbf{x})$ and $\phi(t)$ are each ergodic, that is, their statistics sampled in space and time, respectively, are equal to their ensemble statistics.

Inserting (2.7) into the kinematic equation (2.1) gives

$$\frac{d\mathbf{x}(t)}{dt} = \mathbf{u}[\mathbf{x}(t)]\,\phi(t). \tag{2.8}$$

This nonlinear differential equation is non-autonomous. However, it can be transformed into an autonomous equation by defining the warped time

$$\frac{d\tau(t)}{dt} = \phi(t), \tag{2.9}$$

where $\tau(t = 0) = 0$, and we assume that $\phi(t)$ is positive such that $\tau(t)$ is monotonically increasing with time. By setting $\mathbf{x}(t) = \mathbf{x}'[\tau(t)]$, (2.8) becomes the autonomous differential equation

$$\frac{d\mathbf{x}'(\tau)}{d\tau} = \mathbf{u}[\mathbf{x}'(\tau)]. \tag{2.10}$$

We furthermore assume Lagrangian ergodicity for $v_t(\tau) = \mathbf{u}[\mathbf{x}'(\tau)]$; that is, the statistics sample along a trajectory $\mathbf{x}'(\tau)$ is equal to the statistics sampled across trajectories and to the ensemble statistics analogous to (2.6). This assumption has been found to be valid, for example, for uniform flow through heterogeneous porous media (Le Borgne *et al.* 2008; Hakoun *et al.* 2019; Puyguiraud *et al.* 2019*a*). In order to understand the dynamics of particle motion in this type of separable flow, we can refer to the modelling approach developed for transport in steady random flows (Dentz *et al.* 2016*a*), which, for the convenience of the reader, is summarised in the next subsection.

2.2. *The CTRWs for motion in steady velocity fields*

We consider the case of steady flow, i.e. $\mathbf{u}(\mathbf{x}, t) = \mathbf{u}(\mathbf{x})$ in (2.1). Following Dentz *et al.* (2016*a*), we perform a variable change in (2.1) from time t to travel distance s along a streamline, which is obtained from (2.2).

The subscript t indicates that its values are sampled isochronally along a trajectory. Thus the particle position $\hat{\mathbf{x}}(s)$ and time $t(s)$ satisfy the kinematic equations

$$\frac{d\hat{\mathbf{x}}(s)}{ds} = \frac{\mathbf{u}[\hat{\mathbf{x}}(s)]}{v_s(s)}, \quad \frac{dt(s)}{ds} = \frac{1}{v_s(s)}. \tag{2.11}$$

The Lagrangian speed $v_s(s) = |\mathbf{u}[\mathbf{x}(s)]|$ is sampled equidistantly in space along a trajectory. These kinematic equations describe particle motion in continuous space and time. For ergodic velocity fields – i.e. if the full velocity statistics can be sampled in space (Eulerian), and in time along streamlines (Lagrangian) – the distribution $p_t(v)$ of $v_t(t)$ is equal to the distribution $p_e(v)$ of Eulerian speeds $v_e(\mathbf{x}) = |\mathbf{u}(\mathbf{x})|$:

$$p_t(v) = p_e(v). \tag{2.12}$$

The distribution $p_s(v)$ of $v_s(s)$ is related to $p_t(v)$ and thus to $p_e(v)$ by flux-weighting as

$$p_s(v) = \frac{v p_e(v)}{\langle v_e \rangle}, \tag{2.13}$$

where $\langle v_e \rangle$ denotes the average Eulerian speed. In general, the Lagrangian speed distributions $p_t(v)$ and $p_s(v)$ evolve in time or space towards their respective stationary distributions $p_e(v)$ and $p_s(v)$, depending on the initial speed distribution $p_0(v)$, as discussed in detail in Dentz *et al.* (2016*a*). The initial particle velocity is denoted by $v_s(s = 0) = v_0$.

The velocity process $\{v_s(s)\}$ along trajectories has been modelled as a stationary Markov process characterised by the correlation length ℓ_c and the speed distribution $p_s(v)$. This approach renders particle motion the time-domain random walk (TDRW)

$$\hat{x}(s + ds) = \hat{x}(s) + \frac{ds}{\chi}, \quad t(s + ds) = t(s) + \frac{ds}{v_s(s)}, \tag{2.14}$$

where χ is the advective tortuosity, which is defined by $\langle v_e \rangle / \langle v_1 \rangle$. The velocity series $\{v_s(s)\}$ can be modelled as the Bernoulli process (Dentz *et al.* 2016*a*)

$$v_s(s + ds) = v_s(s)\,\zeta(s) + \nu(s)\,[1 - \zeta(s)], \tag{2.15}$$

where $\zeta(s)$ is a Bernoulli variable that is $\zeta(s) = 1$ with probability $\exp(-ds/\ell_c)$, and $\zeta(s) = 0$ with probability $1 - \exp(-ds/\ell_c)$. The Markov process has also been modelled based on Gaussian copulas (Dentz & Hyman 2023), or in terms of empirical transition probabilities (Le Borgne *et al.* 2008; Sherman *et al.* 2021). The evolution of the speed distribution $\hat{p}_s(v, s)$ with travel distance is given by

$$\frac{\partial \hat{p}_s(v, s)}{\partial s} = \frac{1}{\ell_c} \left[p_s(v) - \hat{p}_s(v, s) \right], \tag{2.16}$$

for the initial speed distribution $\hat{p}_s(v, s = 0) = p_0(v)$. It evolves towards the steady-state distribution $p_s(v)$ exponentially fast on the scale ℓ_c. For $p_0(v) = p_s(v)$, it is constant, i.e. $\hat{p}_s(v, s) = p_s(v)$. The streamwise particle position $x(t)$ is thus given by $x(t) = \hat{x}[s_t]$, where $s_t = \max(s \mid t(s) \leqslant t)$.

Coarse-graining the TDRW given by (2.14) on the correlation scale ℓ_c gives the CTRW

$$\hat{x}_{n+1} = \hat{x}_n + \frac{\ell_c}{\chi}, \quad t_{n+1} = t_n + \tau_n, \tag{2.17}$$

where the transition time is $\tau_n = \ell_c / v_n$, and $v_n = v_s(s_n)$. For $n \geqslant 1$, the τ_n are identical independent random variables whose distribution $\psi(t)$ is given in terms of the Eulerian speed distribution $p_e(v)$ by

$$\psi(t) = \frac{\ell_c^2 \, p_e(\ell_c/t)}{\langle v_e \rangle t^3}. \tag{2.18}$$

For the first CTRW step, i.e. for $n = 0$, the transition time distribution $\psi_0(t)$ is given in term of the initial speed distribution $p_0(v)$ as

$$\psi_0(t) = \frac{\ell_c \, p_0(\ell_c/t)}{t^2}. \tag{2.19}$$

The particle position $x(t)$ in this coarse-grained framework is given by $x(t) = x_{n_t}$, where $n_t = \max(n \,|\, t_n \leqslant t)$. For a steady-state velocity distribution $p_s(v) \propto v^{\alpha - 1}$, the long time behaviours of the displacement mean and variance are given by (Dentz & Hyman 2023)

$$\langle x(t) \rangle = \langle v_e \rangle t, \quad \sigma^2(t) = \langle [x(t) - \langle x(t) \rangle]^2 \rangle \propto t^{3-\alpha}. \tag{2.20}$$

For space–time separable velocity fields, these equations describe the evolution of the displacement mean and variance with $\tau(t)$ replacing t in (2.20).

3. Non-separable random velocity fields

We discuss the case of a non-separable random velocity field, i.e. the fluid velocity $\mathbf{u}(\mathbf{x}, t)$ is characterised by intrinsically coupled space and time variability as defined in § 2.1.1. The distance $s(t)$ travelled by a fluid particle along a pathline of this flow is given by (2.2). Performing the variable transform $t \to s$ in (2.1), we obtain the following system of equations for particle position $\hat{\mathbf{x}}(s)$ and time $t(s)$ with distance s along the pathline as

$$\frac{d\hat{\mathbf{x}}(s)}{ds} = \frac{\mathbf{u}[\hat{\mathbf{x}}(s), t(s)]}{v_s[s, t(s)]}, \quad \frac{dt(s)}{ds} = \frac{1}{v_s[s, t(s)]}, \tag{3.1}$$

where the Lagrangian speed is here defined as $v_s[s, t(s)] \equiv |\mathbf{u}[\mathbf{x}(s), t(s)]|$. Figure 1 illustrates example trajectories $x(t)$ and speed series $v_t(t)$ in the one-dimensional space ($\kappa = \infty$), time ($\kappa = 0$) and space–time ($\kappa = 10$) variable flow fields $u(x, t)$ defined in § 3.3. The trajectories for the steady flow field clearly exhibit the intermittent nature of velocity transitions along a pathline. For the time variable flow, the speed series exhibits a regular random structure characterised by the correlation scale τ_c. The space–time variable flow decorrelates on the correlation scale τ_c but displays intermittent behaviour below this time scale analogous to the case of steady flow.

To address the problem of intermittency observed in figure 1 for finite κ, we introduce the new sampling variable $r = r(s, t)$ along a pathline, and write the Lagrangian speed $\hat{u}[s, t(s)]$ in terms of this variable as

$$v_s[s, t(s)] \equiv v_r(r[s, t(s)]). \tag{3.2}$$

Furthermore, we note that $\mathbf{x}(t) = \hat{\mathbf{x}}[s(t)]$ and $t = t[s(t)]$, which implies $|\mathbf{u}[\mathbf{x}(t), t]| = |\mathbf{u}(\hat{\mathbf{x}}[s(t)], t)|$, thus by using (3.2), we have

$$|\mathbf{u}[\mathbf{x}(t), t]| = v_s[s(t), t] = v_r(r[s(t), t]). \tag{3.3}$$

The sampling variable r is chosen such that the sequence of Lagrangian particle speeds $\{v_r(r)\}$ can be described as a stochastic process with short memory, i.e. as a Markov process. Note that this is possible only for space–time ergodic velocity fields, i.e. velocity fields for which velocity sampling along a pathline in space or time allows us to access the
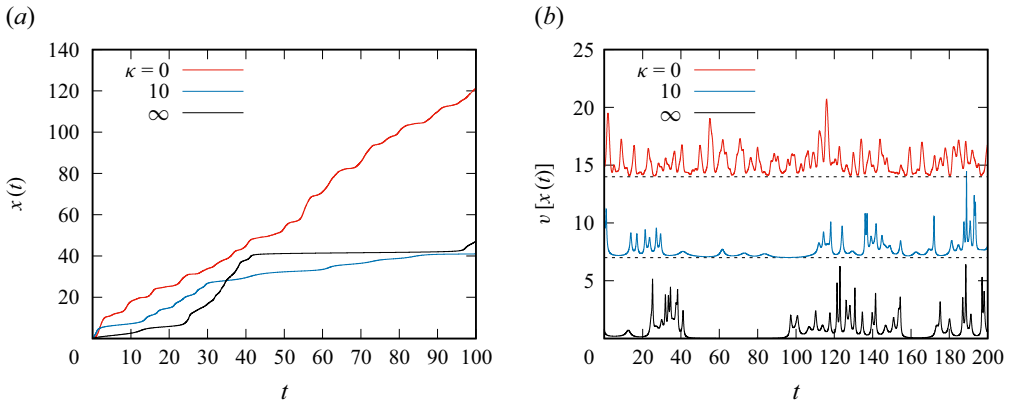
Figure 1. (*a*) Trajectories and (*b*) Lagrangian-in-time speed series for particle motion in multi-Gaussian flow fields with $\kappa = \infty$ ($\tau_c = 1$, black), $\kappa = 0$ ($\ell_c = 1$, red), and $\kappa = 10$ (blue). Times and lengths are given in arbitrary units. One can clearly see the intermittent character of particle motion for the spatially varying flow ($\kappa = \infty$), and the spatio-temporally varying flow below the correlation time.

same (full) velocity spectrum. Under these conditions, the variability of the Lagrangian speed in both distance s and time t along a pathline may be framed in terms of the sampling variable r only via the Lagrangian speed $v_r(r)$, which is characterised by a single correlation scale.

In order to further investigate how r varies with s and t, we analyse the relationship between the increments $\mathrm{d}r$, $\mathrm{d}s$ and $\mathrm{d}t$ along a pathline. They satisfy the identity

$$\mathrm{d}r = \frac{\partial r}{\partial s}\,\mathrm{d}s + \frac{\partial r}{\partial t}\,\mathrm{d}t. \tag{3.4}$$

From this, we can write the space and time increments as

$$\mathrm{d}s = \frac{v(r)\,\mathrm{d}r}{\dfrac{\partial r}{\partial s}\,v_r(r) + \dfrac{\partial r}{\partial t}}, \quad \mathrm{d}t = \frac{\mathrm{d}s}{v_r(r)}, \tag{3.5}$$

where we used

$$\frac{\mathrm{d}s(t)}{\mathrm{d}t} = v_s[s(t),t] = v_r(r[s(t),t]), \quad \frac{\mathrm{d}t(s)}{\mathrm{d}s} = \frac{1}{v_r(r[s,t(s)])}. \tag{3.6}$$

The space and time increments in (3.5) vary according to the local particle speed $v_r(r)$ and the partial derivatives of $r(s,t)$. The Lagrangian speed $v_s[s,t(s)] = v_r(r[s,t(s)])$ changes with respect to both the intrinsic time fluctuations and spatial fluctuations of the underlying velocity field $\mathbf{u}(\mathbf{x},t)$. Hence the Lagrangian speed is randomly reset along the pathline by a combination of spatial variability and intrinsic temporal variability as illustrated in figure 1. When the Lagrangian speed is large, this speed tends to decorrelate due to spatial variability of $\mathbf{u}(\mathbf{x},t)$, whereas decorrelation due to temporal variability of $\mathbf{u}(\mathbf{x},t)$ dominates at small speeds. In accordance with this, the sampling function $r[s,t(s)]$ is defined such that it counts the number of reset events at distance s along a pathline. We consider here velocity fields, for which the reset events in space and time occur independently of each other, and on the constant space and time scales ℓ_c and τ_c, which is a requirement for the flow fields to be space–time ergodic, as discussed in § 2.1.1.
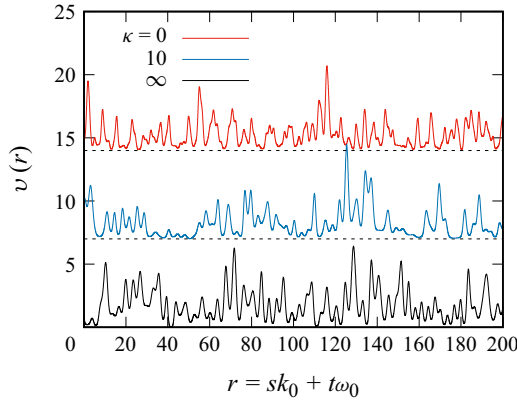
Figure 2. The same Lagrangian speed series as in figure 1, here as a function of the new sampling variable r defined by (3.7). The intermittent patterns observed for $\kappa = 10$ and ∞ are removed.

That is, the reset events in space and time can be approximated as constant rate processes, thus the number of reset events is counted by

$$r(s, t) = sk_0 + t\omega_0, \tag{3.7}$$

where $k_0 = 1/\ell_c$ is the frequency of velocity changes in space, and $\omega_0 = 1/\tau_c$ in time. In this case, the partial derivatives in (3.5) are constant, and the spatial, temporal and sampling increments are all simply linked via the Lagrangian speed $v_r(r)$. Figure 2 shows the same speed series as in figure 1 plotted versus the new sampling variable r. One can clearly see how the intermittent patterns are removed. In the following, we analyse the relation between the speed statistics sampled in r, s and t along pathlines.

3.1. *Lagrangian velocity statistics*

We discuss the Lagrangian speed statistics under the different sampling modes, i.e. sampling in t, s and r. The speed distribution obtained by temporal sampling along streamlines is given by (2.6). As outlined in § 2.1.1, we assume Lagrangian ergodicity, hence $p_t(v) = p_\ell(v) = p_e(v)$. The speed distribution for equidistant sampling along a pathline is defined by

$$p_s(v) = \lim_{L \to \infty} \frac{1}{L} \int_0^L \mathrm{d}s \, \delta(v - |\mathbf{u}[\hat{\mathbf{x}}(s), t(s)]|). \tag{3.8}$$

It is related to $p_t(v) = p_e(v)$ by velocity weighting, which can be seen by replacing $\mathrm{d}s \to v \, \mathrm{d}t$ in (3.8). Thus we obtain

$$p_s(v) = \frac{v \, p_e(v)}{\langle v_e \rangle}, \tag{3.9}$$

where $\langle v_e \rangle$ is the Eulerian mean flow speed. The Lagrangian speed distribution $p_r(v)$ for sampling in r along a pathline is defined as

$$p_r(v) = \lim_{R \to \infty} \frac{1}{R} \int_0^R \mathrm{d}r \, \delta[v - v_r(r)]. \tag{3.10}$$

In order to determine the relation of $p_r(v)$ with the Eulerian speed distribution $p_e(v)$, we write (2.6) as

$$p_t(v) = \lim_{T \to \infty} \frac{1}{T} \int_0^T dt \, \delta[v - v_r(r[s(t), t])], \tag{3.11}$$

where we used (3.3). We furthermore use (3.7) in order to perform the variable transform $t \to r[s(t), t] = s(t) \, k_0 + t\omega_0$. The differential is given by $dr = k_0 \, v_r(r) \, dt + \omega_0 \, dt$, where we used (3.6) to express $ds(t)/dt$ as $v_r(r)$. Using this variable change in (3.10), we obtain the following relation between $p_r(v)$ and the Eulerian speed distribution $p_e(v)$:

$$p_r(v) = \frac{k_0 v + \omega_0}{k_0 \langle v_e \rangle + \omega_0} p_e(v), \tag{3.12}$$

where we used that $p_e(v) = p_t(v)$. This relation allows us to express the mean of the r-Lagrangian velocity $\langle v_r \rangle$ in terms of the statistics of the Eulerian velocity v_e, and vice versa:

$$\langle v_r \rangle = \frac{k_0 \langle v_e^2 \rangle + \omega_0 \langle v_e \rangle}{k_0 \langle v_e \rangle + \omega_0}, \quad \langle v_e \rangle = \frac{1 - \omega_0 \left\langle (k_0 v_r + \omega_0)^{-1} \right\rangle}{k_0 \left\langle (k_0 v_r + \omega_0)^{-1} \right\rangle}. \tag{3.13}$$

3.2. *The TDRWs*

The set of equations (3.5) constitutes a coupled TDRW because the space and time increments are intrinsically coupled via the sampling parameter $r(s, t)$. To demonstrate application of this approach, in this subsection we consider a Bernoulli process for the velocity evolution with r, and formulate particle motion in terms of a stochastic TDRW based on this process. We then coarse-grain the resulting equations in order to obtain a coupled CTRW.

3.2.1. *Stochastic TDRW*

Using the explicit form (3.7) in the system of equations (3.5), we obtain the stochastic TDRW

$$\frac{ds(r)}{dr} = \frac{v_r(r)}{k_0 \, v_r(r) + \omega_0}, \quad \frac{dt(r)}{dr} = \frac{ds(r)}{dr} \frac{1}{v_r(r)}. \tag{3.14}$$

We model $v_r(r)$ as the Bernoulli process

$$v_r(r + dr) = v_r(r) \, [1 - \zeta(r)] + \zeta(r) \, \nu(r), \tag{3.15}$$

where the random variables $\nu(r)$ are independent and identically distributed according to $p_r(v)$. The $\zeta(r)$ are distributed according to

$$p_\zeta(z) = \exp\left(-\frac{dr}{r_c}\right) \delta(z) + \left[1 - \exp\left(-\frac{dr}{r_c}\right)\right] \delta(z - 1), \tag{3.16}$$

where r_c is the correlation distance of $v_r(r)$. The process (3.15) is a mean reverting process that guarantees that $v_r(r)$ converges towards its steady-state distribution $p_r(v)$ for any initial distribution $p_0(v)$.

3.2.2. *Coupled CTRW*

We coarse-grain (3.14) on the correlation scale r_c of $v_r(r)$, and set $r_n = nr_c$, $s_n = s(r_n)$ and $v_n = v_r(r_n)$. With these definitions, we obtain the following discrete set of equations:

$$s_{n+1} = s_n + \xi_n, \quad \xi_n = \frac{v_n r_c}{k_0 v_n + \omega_0}, \tag{3.17a}$$

$$t_{n+1} = t_n + \tau_n, \quad \tau_n = \frac{\xi_n}{v_n}. \tag{3.17b}$$

This system of equations constitutes a coupled CTRW for the evolution of the Lagrangian speed along a pathline. In the limit $k_0 \to 0$, i.e. for an infinite variability length scale, one recovers the discrete time random walk with constant temporal increment $\tau_n = r_c/\omega_0$.

It is illustrative to define a local Kubo number $\kappa_n \equiv v_n k_0/\omega_0 = v_n \tau_c/\ell_c$ for each step in the coupled CTRW. In the limit of small local Kubo number $\kappa_n \ll 1$ (corresponding to small velocities $v_n \ll \ell_c/\tau_c$), the temporal and spatial time steps in (3.17) are controlled by temporal decorrelation

$$\lim_{\kappa_n \to 0} \tau_n = r_c \tau_c, \quad \lim_{\kappa_n \to 0} \xi_n = r_c \tau_c v_n, \tag{3.18}$$

whereas for large local Kubo number $\kappa_n \gg 1$, the temporal and spatial time steps are controlled by spatial decorrelation

$$\lim_{\kappa_n \to \infty} \tau_n = r_c \ell_c/v_n \quad \lim_{\kappa_n \to \infty} \xi_n = r_c \ell_c. \tag{3.19}$$

For intermediate Kubo numbers, $\kappa_n \sim 1$, decorrelation occurs via a competition of spatial and temporal decorrelation, with increments described by (3.17).

In the general case of finite k_0 and ω_0, the joint distribution of transition lengths and times (ξ_n, τ_n) can be defined by

$$\psi_n(x, t) = \left\langle \delta \left(x - \frac{v_n r_c}{k_0 v_n + \omega_0} \right) \delta \left(t - \frac{x}{v_n} \right) \right\rangle. \tag{3.20}$$

The average over v_n can be executed explicitly, which gives

$$\psi_n(x, t) = \frac{r_c}{t^2} p_n(x/t) \delta(k_0 x + \omega_0 t - r_c), \tag{3.21}$$

where $p_n(v) = p_0(v)$ for $n = 0$, and $p_n(v) = p_r(v)$ for $n > 0$. The marginal transition length distribution is given by

$$\rho(s) = \frac{r_c \omega_0}{(r_c - k_0 s)^2} p_n[s\omega_0/(r_c - k_0 s)] H(r_c - k_0 s), \tag{3.22}$$

where the Heaviside function $H(r)$ indicates that, as for the steady flow, the transition length cannot be larger than $r_c \ell_c$. The marginal transition time distribution is

$$\psi(t) = \frac{r_c}{k_0 t^2} p_n[(r_c - \omega_0 t)/k_0 t] H(r_c - \omega_0 t), \tag{3.23}$$

where in this case, as for spatially homogeneous flow, the Heaviside function restricts the transition times to $t < r_c \tau_c$. The coupled CTRW given by (3.17) is equivalent to the following generalised master equation for the distribution $p(s, t)$ of particle positions $s(t)$ (Berkowitz *et al.* 2006):

$$\frac{\partial p(s, t)}{\partial t} = \int \mathrm{d}s' \int_0^s \mathrm{d}s' \, \mathcal{K}(s - s', t - t') \, p(s', t') - \int_0^s \mathrm{d}s' \, \mathcal{K}(s - s') \, p(s, t'), \tag{3.24}$$

where the memory kernels $\mathcal{K}(s, t)$ and $\mathcal{K}(t)$ are defined in Laplace space as

$$\mathcal{K}^*(s, \lambda) = \frac{\lambda \, \psi^*(s, \lambda)}{1 - \psi^*(\lambda)}, \quad \mathcal{K}^*(\lambda) = \int \mathrm{d}s \, \mathcal{K}^*(s, \lambda). \tag{3.25}$$

This type of generalised master equation describes the evolution of particle distribution in fractured media (Berkowitz & Scher 1998; Comolli & Dentz 2017), Levy walks of light in disordered optical materials (Barthelemy *et al.* 2008).

3.3. *Dispersion in one-dimensional random flows*

In order to illustrate the concepts developed in the previous subsections, we consider tracer motion in one-dimensional positive random flow fields $u(x, t) > 0$:

$$\frac{\mathrm{d}x(t)}{\mathrm{d}t} = u[x(t), t], \tag{3.26}$$

where the distance $s(t)$ along a pathline is trivially equal to $x(t)$. The flow fields are generated as positive multi-Gaussian spatio-temporal random fields with marginal distribution $p_u(v)$. A realisation of the target random field $u(x, t)$ is then obtained by the transform

$$u(x, t) = P_u^{-1}\{\Phi[f(x, t)]\}, \tag{3.27}$$

where $P_u(v)$ is the cumulative velocity distribution associated with $p_u(v)$, and $P_u^{-1}(u)$ is its inverse. The function $\Phi(f)$ is the cumulative unit Gaussian distribution, and $f(x, t)$ is a multi-Gaussian random field that is generated by a spectral method following Kraichnan (1970), as outlined in Appendix A. The ensemble mean of $f(x, t)$ is zero, and its covariance function is Gaussian:

$$\langle f(x, t)\, f(x', t')\rangle = \exp\left[-\frac{(x - x')^2}{2\ell_c^2} - \frac{(t - t')^2}{2\tau_c^2}\right], \tag{3.28}$$

where ℓ_c and τ_c are the correlation length and time, respectively. We consider here a Gamma distribution for $p_u(v)$,

$$p_u(v) = \left(\frac{v}{v_c}\right)^{\alpha-1} \frac{\exp(-v/v_c)}{v_c\,\Gamma(\alpha)}, \tag{3.29}$$

where v_c is a characteristic velocity scale. In the following, we compare the dispersion behaviour in spatial, temporal and spatio-temporal random flows, where spatial random flows correspond to the limit $\tau_c \to \infty$, and temporal random flow to $\ell_c \to \infty$. We first define the CTRWs corresponding to each of these scenarios. Then we study the evolution of the displacement mean and variance in these flow fields, and compare them to the estimates of the corresponding coupled CTRWs. Note that this model flow is ergodic in space and time, i.e. both space and time sampling of velocity gives the same velocity statistics $p_u(v)$.

3.3.1. *Velocity statistics*
For particle motion under spatio-temporal velocity fluctuations, (3.26) can be written as

$$\frac{\mathrm{d}x(t)}{\mathrm{d}t} = v_r(r[x(t), t]), \tag{3.30}$$

where we used (3.3). The r-Lagrangian velocity distribution is $p_r(v) = p_u(v)$. Thus from (3.12), for the Eulerian velocity distribution we obtain

$$p_e(v) = \frac{k_0\langle v_e\rangle + \omega_0}{k_0 v + \omega_0}\, p_u(v). \tag{3.31}$$

Coarse-grained particle motion satisfies the correlated CTRW given by the system of equations (3.17). The initial velocity distribution for this CTRW is $p_0(v) = p_u(v)$, which is not equal to the steady-state distribution. This implies that the mean particle velocity evolves from the initial value $\langle v_s\rangle$ towards the steady-state velocity $\langle v_e\rangle$.

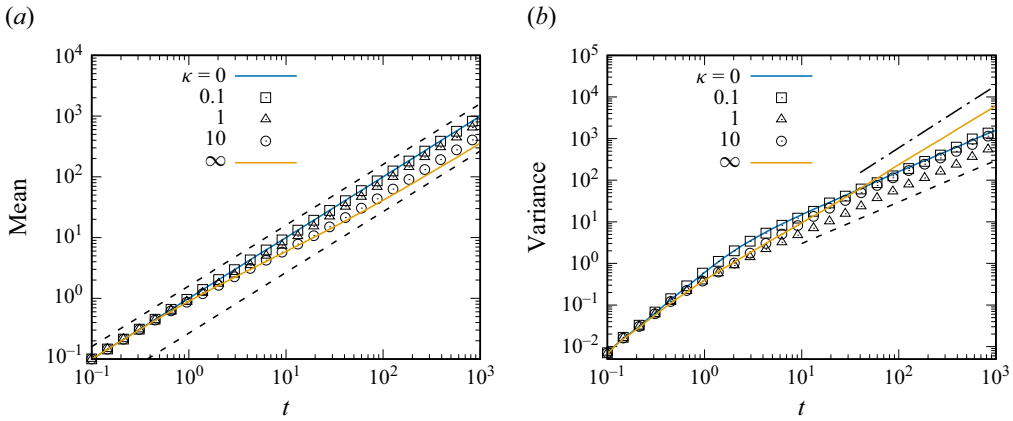Figure 3. Displacement (*a*) mean and (*b*) variance obtained from the numerical solution of (3.26) in Gamma-distributed multi-Gaussian flow fields for $\alpha = 3/2$ with blue solid line for $\kappa = 0$, squares for $\kappa = 0.1$, triangles for $\kappa = 1$, circles for $\kappa = 10$, and orange solid line for $\kappa = \infty$. The dashed lines indicate linear scaling with time, the dash-dotted line the scaling $t^{3-\alpha}$.

For infinite κ, $p_r(v) = p_s(v)$. Expression (3.31) for the Eulerian speed distribution reduces to

$$p_e(v) = \frac{p_u(v) \langle v_e \rangle}{v}, \tag{3.32}$$

where the Eulerian mean $\langle v_e \rangle$ is equal to the harmonic mean of $p_r(v)$:

$$\langle v_e \rangle = \frac{1}{\langle v_r^{-1} \rangle}. \tag{3.33}$$

The initial particle velocity distribution here is $p_0(v) = p_s(v)$, i.e. it is not steady. Thus the velocity statistics need to evolve towards their steady state. The model for $\kappa = \infty$ has been analysed in Dentz *et al.* (2016*a*).

For $\kappa = 0$, i.e. for temporal random flow, the Lagrangian-in-time velocity distribution is $p_t(v) = p_u(v)$, thus the Eulerian velocity probability density function is $p_e(v) = p_u(v)$. The initial velocity distribution is $p_0(v) = p_e(v)$, i.e. it is equal to the steady-state distribution. Therefore, the mean particle velocity is constant and equal to $\langle v_e \rangle$.

3.3.2. *Dispersion behaviour*

Figure 1 shows example trajectories and velocity series for $\kappa = \infty$, 0 and 10. For $\kappa = \infty$, i.e. for spatial random flow, the trajectory is characterised by long periods of time within the same neighbourhood. Analogously, the velocity series is intermittent with long periods at low velocities. For $\kappa = 0$, i.e. temporal random flow, the velocity series is not intermittent, and varies on the fluctuation time scale τ_c. The trajectory fluctuates on the same time scale. For $\kappa = 10$, long periods at low velocities are interrupted due to the temporal resetting of the flow velocity, and the persistent patterns observed for $\kappa = \infty$ are not present here.

These features are also reflected in the behaviours of the displacement mean and variance shown in figure 3. For $\kappa = 0$, the mean evolves linearly with time as $\langle v_e \rangle t$ because the initial condition is stationary, i.e. $p_0(v) = p_e(v)$. For $\kappa = 1$ and $\kappa = \infty$, the mean evolves linearly with slope $\langle v_0 \rangle$ at short times, and crosses over to a linear behaviour with slope $\langle v_e \rangle$ at increasing time. For all cases, the initial slope is the same because they share
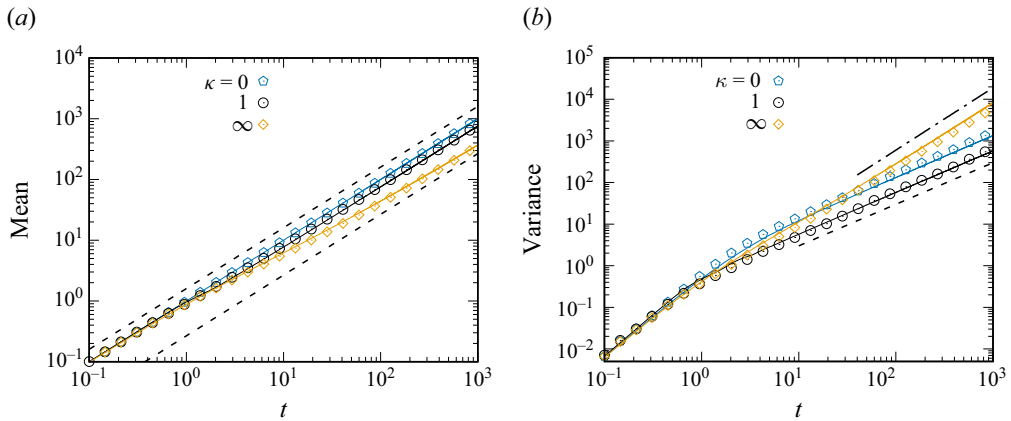
(a)

(b)

Figure 4. Displacement (*a*) mean and (*b*) variance with blue for $\kappa = 0$, black for $\kappa = 1$, and orange for $\kappa = \infty$. Symbols represent particle tracking in the Gamma-distributed multi-Gaussian flow model for $\alpha = 3/2$, and lines represent the corresponding CTRW model. The dashed lines indicate linear scaling with time, the dash-dotted line the scaling $t^{3-\alpha}$.

the same initial velocity distribution $p_0(v) = p_u(v)$. The long-time evolution for $\kappa = \infty$ is slower than for $\kappa = 1$, which in turn is slower than for $\kappa = 0$. This is due to the fact that the mean velocity in steady state is decreasing with increasing κ. The displacement variance for $\kappa = \infty$ shows the characteristic anomalous dispersion behaviour with $\sigma^2(t) \sim t^{3-\alpha}$ as a consequence of memory effects due to the persistence of low velocities in time. For decreasing κ, this persistence is destroyed due to temporal velocity resetting, and the dispersion behaviour becomes normal for times larger than the reset time scale τ_c.

The coupled CTRW model quantifies the salient features of the evolution of particle dispersion for all velocity models as shown in figure 4. The early and late time regimes of displacement mean and variance, and the cross-overs between them, are well reproduced by the model. The details of the cross-over behaviours depend on the type of Markov model used for the evolution of $v_r(r)$. Here, for the sake of simplicity, we employ the Bernoulli process given by (3.15), which may explain the slight discrepancies between the CTRW model and the direct numerical simulations. Alternative velocity Markov models have been discussed in Hakoun *et al.* (2019), Sherman *et al.* (2021) and Dentz & Hyman (2023).

4. Separable random velocity fields

In this section, we derive the CTRW formulation corresponding to particle motion in the space–time separable velocity field (2.7). As shown in § 2.1.2, the kinematic equation for the particle position can be transformed into an autonomous differential equation by defining the warped time $\tau(t)$ given by (2.9). Thus following § 2.2, we first formulate a CTRW in warped time. Then we probe the dispersion behaviour in the separable velocity field for a one-dimensional random flow, and contrast it with the predictions of the warped time CTRW.

4.1. *The CTRW with warped time*

Starting from (2.10), the streamwise particle position $\hat{x}(s)$ can be quantified by the CTRW formalism of § 2.2 by replacing $t \to \tau$:

$$\hat{x}(s + \mathrm{d}s) = \hat{x}(s) + \frac{\mathrm{d}s}{\chi}, \quad \tau(s + \mathrm{d}s) = \tau(s) + \frac{\mathrm{d}s}{v_s(s)}. \tag{4.1}$$

The speed series $v_s(s)$ is modelled by the stationary Markov process given by (3.15). The streamwise position $x'(\tau)$ at warped time τ is now given by $x'(\tau) = \hat{x}(s_\tau)$, where $s_\tau = \max(s \mid \tau(s) \leqslant \tau)$. It describes a CTRW. In analogy to § 3.1, coarse-graining (4.1) on the correlation scale ℓ_c gives

$$\hat{x}_{n+1} = \hat{x}_n + \frac{\ell_c}{\chi}, \quad \tau_{n+1} = \tau_n + \frac{\ell_c}{v_n}, \tag{4.2}$$

where the advective tortuosity χ is defined following (2.14). The streamwise particle position at τ is given by $x'(\tau) = \hat{x}_{n_\tau}$, where $n_\tau = \max(n \mid \tau_n \leqslant t)$.

The streamwise particle position $x(t)$ is given in terms of $x'(\tau)$ by

$$x(t) = x'[\tau(t)]. \tag{4.3}$$

The warped time $\tau(t)$ at the clock time t is given by (2.9), which represents a stochastic process with the characteristic fluctuation time scale τ_c. The temporal stochastic process is ergodic. Thus for $t \gg \tau_c$, we can approximate $\tau(t)$ by

$$\tau(t) = t \left[\frac{1}{t} \int_0^t \mathrm{d}t' \, \phi(t) \right] \approx t \langle \phi(t) \rangle. \tag{4.4}$$

Due to the ergodicity of $\phi(t)$, the quality of this approximation increases with time. Thus for times $t \gg \tau_c$, the transport behaviour for the separable random velocity field is the same as for the corresponding steady random velocity field. This is consistent with the experimental observations of Nissan *et al.* (2017) and Elhanati *et al.* (2023), who observe the same type of non-Fickian transport behaviours for transport in temporally variable and steady porous media flow.

4.2. *Dispersion in one-dimensional separable random flows*

In order to illustrate the transport behaviour in a separable random flow field, we consider tracer motion in a one-dimensional random flow that is given by

$$u(x, t) = u(x) \, \phi(t), \tag{4.5}$$

where $u(x)$ is a multi-Gaussian random field whose marginal is the Gamma distribution given by (3.29). The temporally fluctuating $\phi(t)$ is a multi-Gaussian stochastic process whose marginal is the log-normal distribution, i.e. $f(t) = \ln \phi(t)$ is Gaussian distributed. The numerical generation of $u(x)$ and $f(t)$ follows the methodology described in Appendix A. Its variance is $\sigma_f^2 = 1$ and mean $\mu = -\sigma_f^2/2$, such that the mean is $\langle \phi(t) \rangle = 1$ and the mean square is $\langle \phi(t)^2 \rangle = \exp(\sigma_f^2)$.

Figure 5 shows the displacement mean and variance for separable velocity fields with $\kappa = 0.1$, 1 and 10 compared to their counterparts for the steady velocity field. The mean displacements behave in the same way. In fact, at short times $m(t)$, they are given by

$$m(t) = \langle u \rangle \int_0^t \mathrm{d}t' \langle \phi(t') \rangle = \langle u \rangle t. \tag{4.6}$$

At large times, we obtain by combining (4.4) and (2.20) the linear behaviour

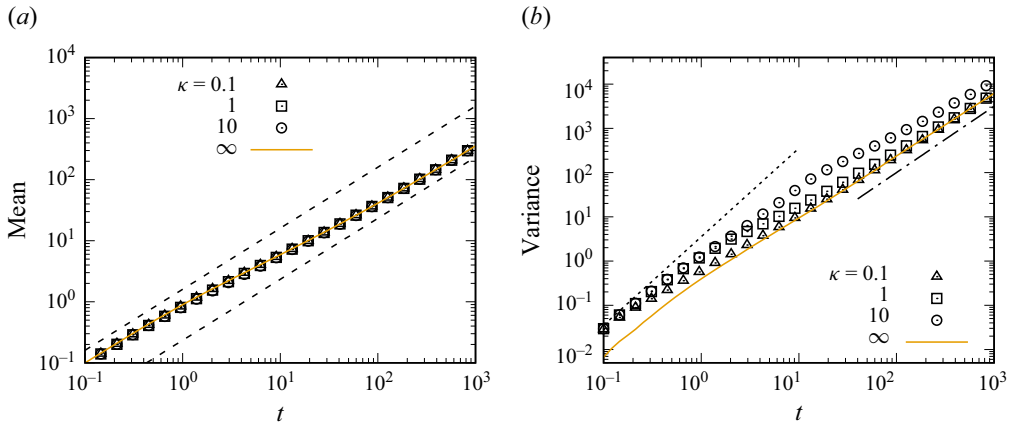$$m(t) = \langle v_e \rangle t. \tag{4.7}$$

(*a*)

(*b*)

Figure 5. Displacement (*a*) mean and (*b*) variance, with triangles for $\kappa = 0.1$, squares for $\kappa = 1$, circles for $\kappa = 10$, and orange lines for $\kappa = \infty$. The dotted lines denote the expected ballistic behaviour at early times. The dashed lines indicate linear scaling with time, the dash-dotted line the scaling $t^{3-\alpha}$.

The displacement variance behaves ballistically at short times, i.e.

$$\sigma^2(t) = \left(\langle u^2 \rangle \langle \phi^2 \rangle - \langle u \rangle^2 \langle \phi \rangle^2 \right) t^2, \tag{4.8}$$

while we obtain for the steady flow field $\kappa(t) = \sigma_u^2 t^2$. For times $t \gg \tau_c$, the displacement variance for the separable velocity fields converges towards the displacement behaviour for the steady velocity field. In fact, based on (4.4) and (2.20) we find that for $\tau(t) \approx t \gg \tau_v$,

$$\sigma^2(t) \propto \langle \tau(t)^{3-\alpha} \rangle \approx t^{3-\alpha} \tag{4.9}$$

because $\langle \phi(t) \rangle = 1$. Figure 5 shows that the numerical data adjust well to the analytical short- and long-time solutions for the displacement mean and variance. While the anomalous long-time behaviour persists, we observe that the displacement variance is larger in the presence of temporal fluctuations than for the corresponding steady flow field. This is in line with Nissan *et al.* (2017) and Elhanati *et al.* (2023), who observe enhanced solute dispersion in porous columns under pressure fluctuation in the direction of the mean flow.

5. Summary and conclusion

We investigate the stochastic dynamics of particle motion in spatio-temporal random flow fields. Unlike for steady random flow, for which particle velocities vary on characteristic length scales that are imprinted in the spatial flow structure, here velocity variability is governed by the competition between spatial and temporal velocity resets along particle paths. We analyse two types of velocity field that are characterised by non-separable and separable space–time fluctuations. In the first type, spatial and temporal fluctuations are intrinsically coupled. We assume that the fields are space–time ergodic, i.e. the same statistics are sampled by the space and time fluctuations. Furthermore, we assume Lagrangian ergodicity, i.e. each particle can sample the full velocity statistics along a pathline. The second type of flow field is separable into spatial and temporally fluctuating random fields. In general, they do not explore the same statistics in space and time, i.e. these fields are not space–time ergodic. For these fields, we assume that that the space and

time fluctuating parts are each ergodic, and the space part fulfils Lagrangian ergodicity in warped time.

For non-separable random flows, the character of particle motion is determined by the Kubo number. For low Kubo numbers, dispersion is dominated by rapid temporal velocity fluctuations, which interrupt episodes of spatially correlated ballistic motion along pathlines, and quickly lead to normal dispersive behaviours characterised by a linear growth of the displacement variance. For large Kubo numbers, temporal velocity reset is slow compared to spatial, and pre-asymptotic dispersion is dominated by ballistic motion over the correlation scale, which, for flow fields with broadly distributed velocities, leads to anomalous dispersion characterised by a nonlinear increase of the displacement variance. Nevertheless, at times larger than the temporal correlation scale, dispersion becomes normal because episodes of particle velocities are interrupted by temporal reset and cannot be arbitrarily long. At intermediate Kubo numbers, dispersion evolves towards normal behaviour, but is smaller than for the temporal random flows due to particle retention at low velocities before the temporal velocity reset. In order to rationalise these behaviours in a stochastic framework, we define a new sampling variable that counts the number of spatial and temporal velocity resets. In this frame, subsequent particle velocities can be considered as independent, and particle velocity series can be quantified as Markov processes, which represents a significant simplification for the analysis of this otherwise complex stochastic processes. We discuss the Lagrangian velocity statistics as a function of the new sampling variables and their relation to the Eulerian velocity statistics. The identified stochastic rules of motion can be cast into the framework of a coupled continuous time random walk (CTRW), i.e. a CTRW for which the time and space increments are intrinsically coupled. The model accounts for the full range of dispersion behaviours at all Kubo numbers. In the limit $\kappa \to \infty$, the CTRW for steady random flows is recovered, and for $\kappa \to 0$, diffusive behaviour characterised by randomly varying space and constant time increments.

While for non-separable random flows dispersion becomes asymptotically Fickian, for space–time separable flows, the same anomalous dispersion behaviour observed for the corresponding steady flow fields persists. That is, for broad distributions of flow velocities, the displacement variance increases in both cases nonlinearly with time. Even though the variances show the same long-time scaling in both cases, they are larger in the presence of temporal flow fluctuations. This is consistent with the experimental observations of Nissan *et al.* (2017) and Elhanati *et al.* (2023) for dispersion in porous media flows under streamwise flow fluctuations. These authors find the same type of anomalous behaviour as for steady porous media flows, but enhanced tracer spreading and broader residence time distributions as in steady flows. The persistence of the steady flow behaviours can be explained by the fact that particle motion in the transient flow can be mapped onto particle motion in a corresponding steady flow field by defining a warped time. In this frame, particle motion obeys CTRW dynamics. Then for ergodic time fluctuations, warped time evolves asymptotically linearly with time, which explains the persistence of anomalous dispersive behaviours.

The two classes of space–time variable flow fields may be relevant for a range of flow scenarios such as dispersion in poroelastic and rigid porous media under fluctuating boundary conditions, and for flows in which particle velocities are reset randomly in both space and time. The resetting may be intrinsic to the flow as, for example, under turbulent flow conditions, or extrinsic to the flow as for particle advection under diffusion. In the latter case, particles may change velocities due to lateral diffusion between streamlines. The coupled CTRW for particle motion can account for broad distributions of space and time scales, and may thus be relevant for the quantification of pair dispersion, for which multiscale interactions can be important. In fact, Levy walk and CTRW approaches have

been used in the past to explain Batchelor and Richardson scalings in pair dispersion (Shlesinger *et al.* 1987; Sokolov *et al.* 2000; Thalabard *et al.* 2014). Our results shed light on the mechanisms of dispersion in spatio-temporal random flows. They show that alternative strategies for the analysis of Lagrangian velocity data and particle trajectories using new sampling variables may facilitate the identification of (hidden) Markov models, and enable the development of reduced-order models for otherwise complex particle dynamics.

Declaration of interests. The authors report no conflict of interest.

Appendix A. Generation of one-dimensional random flow fields

A.1. *Uniform in space, non-uniform in time*

We consider the Gaussian random field

$$f(t) = \sqrt{\frac{2}{N}} \sum_{j=0}^{N} \cos(\omega_j t + \varphi_j), \tag{A1}$$

where the ω_j are independent identically distributed (i.i.d.) random variables distributed according to

$$p_\omega(w) = \frac{\exp(-w^2/2\omega_0^2)}{\sqrt{2\pi\omega_0^2}}. \tag{A2}$$

The phases φ_j are also i.i.d. random variables, which are uniformly distributed in $[0, 2\pi]$. The resulting random field $f(t)$ is Gaussian distributed in the limit $N \to \infty$. Its mean is 0, its variance is 1, and its correlation function is

$$\langle f(t)\, f(t') \rangle = \exp(-\omega_0\, (t - t')^2), \tag{A3}$$

hence the correlation time is $\tau_c = 1/\omega_0$.

A.2. *Uniform in time, non-uniform in space*

We consider the Gaussian random field

$$f(x) = \sqrt{\frac{2}{N}} \sum_{j=0}^{N} \cos(\kappa_j x + \varphi_j). \tag{A4}$$

As above, here the k_j are i.i.d. and follow the Cauchy distribution

$$p_\kappa(k) = \frac{\exp(-k^2/2k_0^2)}{\sqrt{2\pi k_0^2}}. \tag{A5}$$

The resulting flow field is Gaussian with mean 0, unit variance and the Gaussian correlation function

$$\langle f(x) f(x') \rangle = \exp(-k_0^2 (x - x')^2/2). \tag{A6}$$

A.3. *Non-uniform in space and time*

We consider the Gaussian random field

$$f(x, t) = \sqrt{\frac{2}{N}} \sum_{j=0}^{N} \cos(k_j x + \omega_j t + \varphi_j). \tag{A7}$$

The frequencies k_j and ω_j are independent random variables distributed according to (A5) and (A2), respectively. Again, the resulting flow field is Gaussian distributed with mean 0, unit variance, and Gaussian correlation function.

REFERENCES

DE ANNA, P., LE BORGNE, T., DENTZ, M., TARTAKOVSKY, A.M., BOLSTER, D. & DAVY, P. 2013 Flow intermittency, dispersion and correlated continuous time random walks in porous media. *Phys. Rev. Lett.* **110** (18), 184502.

BARTHELEMY, P., BERTOLOTTI, J. & WIERSMA, D.S. 2008 A Lévy flight for light. *Nature* **453** (7194), 495–498.

BERKOWITZ, B., CORTIS, A., DENTZ, M. & SCHER, H. 2006 Modeling non-Fickian transport in geological formations as a continuous time random walk. *Rev. Geophys.* **44** (2), RG2003.

BERKOWITZ, B. & SCHER, H. 1998 Theory of anomalous chemical transport in fracture networks. *Phys. Rev. E* **57** (5), 5858–5869.

CIRPKA, O. & ATTINGER, S. 2003 Effective dispersion in heterogeneous media under random transient flow conditions. *Water Resour. Res.* **39** (9), 1257.

COMOLLI, A. & DENTZ, M. 2017 Anomalous dispersion in correlated porous media: a coupled continuous time random walk approach. *Eur. Phys. J. B* **90** (9), 166.

COMOLLI, A., HAKOUN, V. & DENTZ, M. 2019 Mechanisms, upscaling, and prediction of anomalous dispersion in heterogeneous porous media. *Water Resour. Res.* **55** (10), 8197–8222.

DAGAN, G. 1989 *Flow and Transport in Porous Formations*. Springer.

DENTZ, M., HIDALGO, J.J. & LESTER, D. 2023 Mixing in porous media: concepts and approaches across scales. *Transp. Porous Med.* **146** (1), 5–53.

DENTZ, M. & HYMAN, J.D. 2023 The hidden structure of hydrodynamic transport in random fracture networks. *J. Fluid Mech.* **977**, A38.

DENTZ, M., KANG, P.K., COMOLLI, A., LE BORGNE, T. & LESTER, D.R. 2016*a* Continuous time random walks for the evolution of Lagrangian velocities. *Phys. Rev. Fluids* **1** (7), 074004.

DENTZ, M., LESTER, D.R., LE BORGNE, T. & DE BARROS, F.P.J. 2016*b* Coupled continuous-time random walks for fluid stretching in two-dimensional heterogeneous media. *Phys. Rev. E* **94** (6), 074004.

DJENIDI, L., TARDU, S. & ANTONIO, R.A. 2013 On the ergodicity of grid turbulence. In *Eighth International Symposium on Turbulence and Shear Flow Phenomena*. Begel House Inc.

DE DREUZY, J.-R., CARRERA, J., DENTZ, M. & LE BORGNE, T. 2012 Asymptotic dispersion for two-dimensional highly heterogeneous permeability fields under temporally fluctuating flow. *Water Resour. Res.* **48** (1), W01532.

ELHANATI, D., DROR, I. & BERKOWITZ, B. 2023 Impact of time-dependent velocity fields on the continuum-scale transport of conservative chemicals. *Water Resour. Res.* **59** (9), e2023WR035266.

ENGDAHL, N.B. & AQUINO, T. 2022 Upscaled models for time-varying solute transport: transient spatial-Markov dynamics. *Adv. Water Resour.* **166**, 104271.

FRISCH, U. 1995 *Turbulence: The Legacy of A.N. Kolmogorov*. Cambridge University Press.

GALANTI, B. & TSINOBER, A. 2004 Is turbulence ergodic? *Phys. Lett. A* **330** (3–4), 173–180.

HAKOUN, V., COMOLLI, A. & DENTZ, M. 2019 Upscaling and prediction of Lagrangian velocity dynamics in heterogeneous porous media. *Water Resour. Res.* **55** (5), 3976–3996.

HALLER, G. 2015 Lagrangian coherent structures. *Annu. Rev. Fluid Mech.* **47** (1), 137–162.

HYMAN, J.D., DENTZ, M., HAGBERG, A. & KANG, P.K. 2019 Linking structural and transport properties in three-dimensional fracture networks. *J. Geophys. Res.: Solid Earth* **124** (2), 1185–1204.

KRAICHNAN, R.H. 1970 Diffusion by a random velocity field. *Phys. Fluids* **13** (1), 22–31.

KROMMES, J.A. & SMITH, R.A. 1987 Rigorous upper bounds for transport due to passive advection by inhomogeneous turbulence. *Ann. Phys.* **177** (2), 246–329.

KUBO, R. 1962 Generalized cumulant expansion method. *J. Phys. Soc. Japan* **17** (7), 1100–1120.

LE BORGNE, T., DENTZ, M. & CARRERA, J. 2008 Lagrangian statistical model for transport in highly heterogeneous velocity fields. *Phys. Rev. Lett.* **101** (9), 090601.

LESTER, D.R., DENTZ, M., LE BORGNE, T. & DE BARROS, F.P.J. 2018 Fluid deformation in random steady three-dimensional flow. *J. Fluid Mech.* **855**, 770–803.

MORALES, V.L., DENTZ, M., WILLMANN, M. & HOLZNER, M. 2017 Stochastic dynamics of intermittent pore-scale particle motion in three-dimensional porous media: experiments and theory. *Geophys. Res. Lett.* **44** (18), 9361–9371.

NEUPAUER, R.M., MEISS, J.D. & MAYS, D.C. 2014 Chaotic advection and reaction during engineered injection and extraction in heterogeneous porous media. *Water Resour. Res.* **50** (2), 1433–1447.

NISSAN, A., DROR, I. & BERKOWITZ, B. 2017 Time-dependent velocity-field controls on anomalous chemical transport in porous media. *Water Resour. Res.* **53** (5), 3760–3769.

POPE, S.B. 2000 *Turbulent Flows*. Cambridge University Press.

PUYGUIRAUD, A., GOUZE, P. & DENTZ, M. 2019a Stochastic dynamics of Lagrangian pore-scale velocities in three-dimensional porous media. *Water Resour. Res.* **55** (2), 1196–1217.

PUYGUIRAUD, A., GOUZE, P. & DENTZ, M. 2019b Upscaling of anomalous pore-scale dispersion. *Transp. Porous Med.* **128** (2), 837–855.

REHFELDT, K.R. & GELHAR, L.W. 1992 Stochastic analysis of dispersion in unsteady flow in heterogeneous aquifers. *Water Resour. Res.* **28** (8), 2085–2099.

SAFFMAN, P.G. 1959 A theory of dispersion in a porous medium. *J. Fluid Mech.* **6** (3), 321–349.

SHERMAN, T., ENGDAHL, N.B., PORTA, G. & BOLSTER, D. 2021 A review of spatial Markov models for predicting pre-asymptotic and anomalous transport in porous and fractured media. *J. Contam. Hydrol.* **236**, 103734.

SHLESINGER, M.F., WEST, B.J. & KLAFTER, J. 1987 Lévy dynamics of enhanced diffusion: application to turbulence. *Phys. Rev. Lett.* **58** (11), 1100–1103.

SOKOLOV, I.M., KLAFTER, J. & BLUMEN, A. 2000 Ballistic versus diffusive pair dispersion in the Richardson regime. *Phys. Rev. E* **61** (3), 2717–2722.

THALABARD, S., KRSTULOVIC, G. & BEC, J. 2014 Turbulent pair dispersion as a continuous-time random walk. *J. Fluid Mech.* **755**, R4.

VILLERMAUX, E. 2019 Mixing versus stirring. *Annu. Rev. Fluid Mech.* **51** (1), 245–273.